Available online at www.sciencedirect.com
SCIENCE DIRECT
Polymer 46 (2005) 3472–3480
polymer
www.elsevier.com/locate/polymer

Crystalline structure and phase structure of mLLDPE/LDPE blends

T. Wu[a], Y. Li[b], G. Wu[a,*]

[a]Key Laboratory of Beijing City on 'Preparation and Processing of Novel Polymer Materials', College of Materials Science and Engineering, Beijing University of Chemical Technology, Beijing 100029, People's Republic of China
[b]Department of Chemical Engineering, Institute of Polymer Science and Engineering, Tsinghua University, Beijing 100084, People's Republic of China

Received 4 June 2004; received in revised form 23 December 2004; accepted 24 February 2005
Available online 19 March 2005

Abstract

The crystalline structure and phase structure of metallocene linear low density polyethylene (mLLDPE) and low density polyethylene (LDPE) blends were investigated, using a combination of differential scanning calorimetry (DSC), wide-angle X-ray diffraction (WAXD), and small-angle X-ray scattering (SAXS) techniques. The samples displayed cocrystallization phenomenon for LDPE of 80 wt% in the blends, indicating good compatibility between the two components under this circumstance; as LDPE content decreased, phase separation arose whereas partial cocrystallization still existed in the blends. Over the whole range of weight fractions, the intrinsic crystal structure of mLLDPE does not change with the addition of LDPE, while enhanced orthorhombic crystalline phase were observed as LDPE content increased. The changes in the thickness of interface layer σ_b, dispersed phase size a_c and integral invariant Q further indicate the existence of partial compatibility between the two phases. Irrespective of the phase inversion, the morphology of the dispersed phase is deduced to be in a transitional state from rod-like shape to flakes within the whole proportional range investigated.

Keywords: Metallocene linear low density polyethylene (mLLDPE); Crystalline structure; Phase structure

1. Introduction

Over the past decades, the well understanding of the characteristics of metallocene catalysts [1] as well as their catalyzing mechanism has provided the possibility to design the chain structure of polyethylene at a microscopic molecular level according to the practical performance of products. Consequently, a new range of polyethylene grades, metallocene polyethylene (mPE) with highly regular molecular design has been attained. Compared to conventional polyethylene produced with Ziegler–Natta catalysts, mPE possesses narrow molecular weight distribution (MWD) and narrow comonomer composition distribution, along with strictly controlled side chain length and branching degree [2,3]. It is well known that narrow molecular weight distribution relates to almost non-existence of highly branched polymers, whereas narrow composition distribution of comonomer leads to low melting point and narrow melting point range compared to those of conventional polyethylene [4]. Meanwhile, the content of short branched chains has effect on the elasticity of polymer materials, such as the crystallinity, modulus and rigidity [5]. The particular intermolecular structure mentioned above provide metallocene polyethylene with superior physical and mechanical properties, which could meet the wide application in medical and packaging fields. However, this special structure may also lead to poor processabilities of mPE, comprising high melt viscosities, inferior fluidity and low melt intensity, which result in badly restriction in further application fields.

Among the methods reported to improve the processing of mPE [6–11], one of the most important evolution is using catalysts with different metallocene sites (or mixed catalysts) to widen the MWD of mPE, or to produce polyethylene with a bimodal MWD [12]. Nevertheless, the obtained material is essentially similar to the blend system consisting of two polymer components with identical chemical composition but different molecular weights; therefore, heterogeneous phase structure might exist inside the materials, which result in potential deficiencies and negative effects in many aspects [13]. However, the study

* Corresponding author.
E-mail address: gangwubuct@sina.com (G. Wu).

0032-3861/$ - see front matter © 2005 Elsevier Ltd. All rights reserved.
doi:10.1016/j.polymer.2005.02.084

on polyolefin blends is an expanding field both in academia and industry, therefore a better understanding, characterization and prediction of the blend properties are of importance [14–16]. Due to their similarity in structure, the phase separation and phase behaviors in the melt could not be directly discerned for many commercial blends, for instance, binary pairs of HDPE/LDPE. Moreover, the compatibility, liquid–liquid and liquid–solid phase separation, as well as the subsequently formed highly regular aggregation structure for polyolefin blends could not only have a crucial effect on the melt processing and rheological properties, but also directly affect the final properties of the products [17]. Consequently, the description of the variables concerning polymer crystalline–amorphous phases (for instance, crystallinity, lamellar thickness and amorphous region thickness) on a micromolecular level should be of great interest.

The blends of LDPE and mPE have been well documented (see, for example, Refs. [9,18,19]), mostly concentrating on the investigation of rheological properties, thermal properties and mechanical properties of the blends, and many significative results have been achieved. However, there have not been prior studies using the combination of DSC, WAXD and SAXS to investigate the crystalline structure, phase structure and phase separation of mLLDPE/LDPE blends. In the present study, by means of DSC, WAXD and SAXS analysis, we focus on the blend system of mLLDPE and LDPE with proportional compositions, in the interest of exhibiting the changing tendency in parameters of crystalline structure such as crystallinity and lamellar thickness, as well as the changing tendency in parameters of phase structure (for instance, interface layer thickness σ_b, Porod index α, dispersed phase size a_c, integral invariant Q, etc.). The objective of this paper is to afford a reasonable theoretical correlation for the improvement in processabilities and properties of mLLDPE/LDPE blends.

2. Experimental

2.1. Materials and melt processing

The metallocene linear low density polyethylene (mLLDPE) used was supplied by Exxon Chemical Company as Exceed350D65 grade. Low density polyethylene (LDPE) 0274 was provided by QATAR Petrochemical Co. Ltd. The characterization results of the two materials are listed in Table 1, in which the molecular parameters of materials, M_n, M_w, M_w/M_n, were measured on a PL-210 GPC instrument.

The composition of mLLDPE/LDPE blends is given in Table 2. The blends of varied weight proportions were mixed at 160 °C using a RM-200 rheometer mixer (Harst Technology Development Company, Harbin, China), at a fixed speed of 35 rpm. Then the samples were compression molded at 160 °C for WAXD and SAXS measurements.

2.2. Characterization

Differential scanning calorimetry (DSC) thermograms were measured using a Perkin–Elmer DSC-2C calorimeter. The temperature and heat flow were calibrated before the measurement. All samples were heated from 50 to 150 °C at a rate of 10 °C/min in nitrogen atmosphere, held at 150 °C for 5 min, then cooled down to 50 °C at 10 °C/min.

Wide-angle X-ray diffraction (WAXD) intensity patterns were collected on a D/max 2500 VB2+/Pc diffractometer equipped with a computerized data collection and analytical system. The monochromatized X-ray beam was Cu K_α radiation. The operating condition of the X-ray source was set at a voltage of 40 kV and a current of 200 mA.

Small-angle X-ray scattering (SAXS) data were also collected on a D/max 2500 VB2+/Pc diffractometer using Cu K_α radiation, operated at 40 kV and 200 mA with a 0.02° step size of 2θ from 0.06 to 2.0°. The absolute intensity for $I(S)$ has been evaluated using four slit collimation system, and the mensuration of absolute intensity has been carried out on standard samples.

3. Results and discussion

3.1. DSC analysis of mLLDPE/LDPE blends

As the main phase behavior of crystalline/crystalline polymer blends, the process of crystalline phase separation decides the structure and properties of the blends, and the composition dependence of crystalline phase separation reflects the intermolecular interactions and the dispersion state of the components. Since corresponding information could be obtained by dynamic investigation of crystalline polymers, DSC measurement was employed in the present study to investigate the crystalline phase separation process for mLLDPE/LDPE blends.

The curves of DSC melting and cooling scans for mLLDPE/LDPE blends are plotted in Fig. 1. It can be seen

Table 1
Materials used in this study

Material	Density[a]/(g cm^{-3})	MI[a]/(g 10 min)	$\bar{M}_n$	$\bar{M}_w$	$\bar{M}_w/\bar{M}_n$
mLLDPE	0.917	1.0	43,529	113,030	2.6
LDPE	0.923	2.0	18,382	88,218	4.8

[a] Obtained from the supplier.

Table 2
Composition of mLLDPE /LDPE blends

Blend system	Polymer weight fraction (%)					
mLLDPE/LDPE	100/0	80/20	60/40	40/60	20/80	0/100

that with 80 wt% LDPE content, the two melting peaks almost overlap. Especially, only one single crystallization peak is formed during the cooling process, simultaneously the peak profiles become widened compared to those of the original components, indicating the existence of one type of crystal species. That is to say, cocrystallization of mLLDPE and LDPE occurs. On the other hand, blends of mLLDPE/LDPE-80/20, 60/40, 40/60 show two distinct peaks both in melting and cooling traces, manifesting the occurrence of phase separation. It is reasonable to assume that as the temperature slowly decreases, liquid–liquid and solid–liquid phase separation arises, driving mLLDPE and LDPE chain segments to form their individual rich domains. Consequently, double-peaks were observed in the cooling process. According to Kohji Tashiro et al. [20], the crystallization temperature and peak profile of the polymer blends might be influenced by the lamellar size and the interactions at the boundary between the two lamellae of different species. In addition, the lamellae of one species might be surrounded not only by the amorphous phase of itself but also by the amorphous chains of the other species, for these reasons the crystallization behaviors of each component in the blend system were influenced.

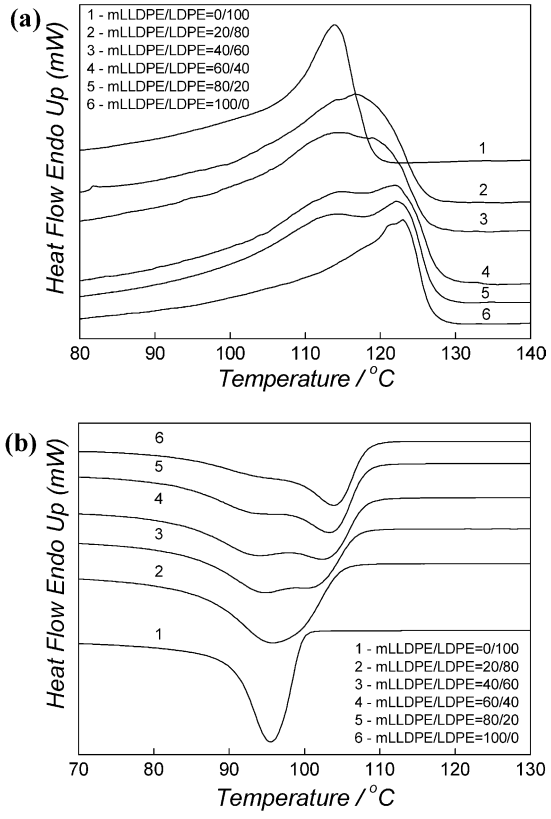

Fig. 1. DSC traces for mLLDPE/LDPE blends: (a) melting process; (b) cooling process.

Based on the parting disposal of corresponding peaks using Peakfit software, Fig. 2 shows the composition dependence of melting and crystallization temperature for mLLDPE/LDPE blends. With the increase of LDPE content, the peak values relating to mLLDPE take on gradually decreasing tendency, whereas the peak values relating to LDPE increase gradually. Therefore, the corresponding peak values come nearer to each other, together with lowered peak height compared to those of the individual components, indicating that there is still a certain degree of cocrystallization in the blends. According to Ref. [21], this phenomenon might be ascribed to the kinetic effects or the thermal retardation in the crystallization process. It should be noted that the discussion mentioned above is in contradiction with the reports of Ref. [9]. In the latter case, single peak was observed only at an 80/20 weight ratio of mLLDPE/LDPE blend. The possible reason might lie in the difference of the molecular weight, molecular weight distribution and the branching degree of the materials used.

3.2. WAXD analysis

In the present study, the intension of the WAXD experiment are two-fold: (1) it is to investigate whether or not the addition of LDPE affect the formation of crystals during crystallization, and (2) it is to investigate whether or not the addition of LDPE affect the amount of crystalline content formed. Fig. 3 illustrates WAXD diffractograms for mLLDPE/LDPE blends. It can be seen that for all samples, the diffractograms exhibit major characteristic crystalline peaks of polyethylene at the scattering angles $2\theta = 21.46 \pm 0.10°$ and $23.70 \pm 0.10°$, which corresponds to the reflection planes at (110) and (200), respectively. This clearly suggests that with the addition of LDPE, the characteristic orthorhombic crystals are retained, namely, the intrinsic crystal structure of mLLDPE has not been influenced. On the other hand, the position, intensity and profiles of the corresponding diffraction peaks of the blends have been changed to some extent, behaving improved diffraction intensity of (110), (200) crystal planes and the amorphous halo (relating scattering angle $2\theta = 19.50 \pm 0.10°$) compared to those of pure mLLDPE.

To eliminate the errors resulted in the preparation and measurement process of the samples, the intensity area (IA) ratios of I_{110} and I_{200} were adopted to figure the changes of diffraction intensities for the blends in Table 3, together with the changes in the ratios of half-peak width β_{110} and

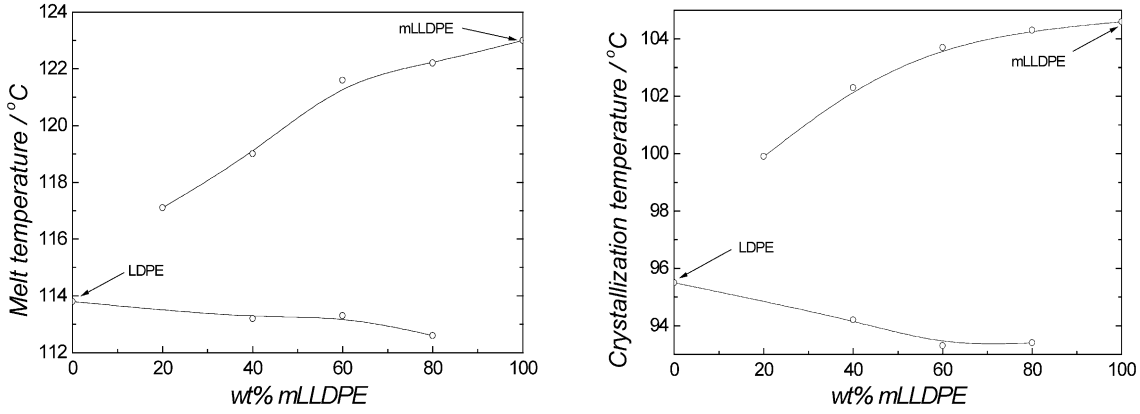

Fig. 2. The composition dependence of melting and crystallization temperature for mLLDPE/LDPE blends (left, melting process; right, cooling process).

β_{200} to make a comparison. As verified by the changes of IA_{110}/IA_{200}, it can be deduced that with the increase of LDPE content, the orthorhombic crystalline phase is enhanced, except for the blend with 80 wt% LDPE content. This may be ascribed to two factors: (1) there are similar crystal characteristics for both pure LDPE and mLLDPE, i.e. orthorhombic lattice, so that this specific crystal structure is retained after the blending, simply slight changes in the parameters of crystal cell occurs; (2) concerning the intermolecular heterogeneity between LDPE and mLLDPE macromolecules (for instance, the difference in average molecular weight and the molecular weight distribution), in the rich domain of one macromolecule, the regular arrangement of the chain segments of the other species might be excluded during crystallization, accordingly the original crystalline thermodynamics state of the given macromolecule is altered. As a result, the crystal size becomes smaller and the crystal perfect degree of the blends increases, accordingly have an effect on the crystallizing process and the finally formed aggregation structure. Concerning the blend with 80 wt% LDPE content, its exceptive lower intensity ratios of IA_{110} and IA_{200} might result from the cocrystallization of mLLDPE and LDPE, which leads to more crystal defects, accordingly decrease the diffraction intensity of characteristic crystalline peaks.

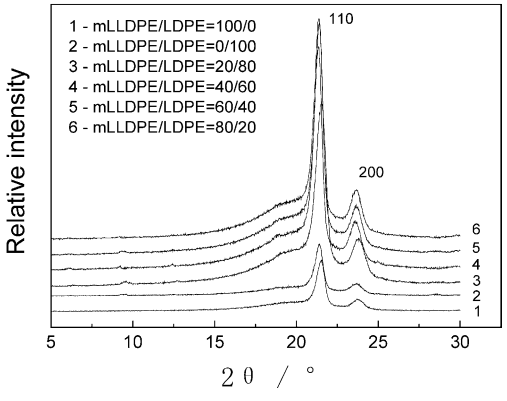

Fig. 3. WAXD patterns of mLLDPE/LDPE blends.

Besides, it should be noted here that although exclusion is the main interactions as discussed above, very low degree of intermolecular adsorption might happen between the similar segments, which is responsible for the formation of partial cocrystallization.

One simple approach to estimate the apparent degree of crystallinity from the WAXD experiment is to compute the integrated intensities of the pattern associated with the crystalline structures and the amorphous halo. It is approximately deemed that the total scattering within a certain region of reciprocal space is independent of the state of aggregation of the materials. The degree of crystallinity χ_c^{WAXD} is therefore expressed by the mass fraction of crystalline aggregates, and can be determined from the WAXD patterns based on the ratio of the integrated intensities under the crystalline peaks to the integrated total intensities, which can be depicted as [22]

$$\chi_c^{WAXD} = \frac{I_c}{I_c + K_x I_a} \tag{1}$$

where I_c is the integrated intensities under the crystalline peaks, I_a is the integrated intensities under the amorphous halo underneath the crystalline reflections, and K_x is the emendatory coefficient.

According to the definition of K_x and the calculation method given in Ref. [22], an amendment was made to the diffraction intensities relating to the crystalline reflection (110), (200) and the amorphous halo, accordingly the WAXD degree of crystallinity χ_c^{WAXD} for all the samples could be obtained quantitatively by Eq. (2) as the following:

$$\chi_c^{WAXD} = \frac{I_{110} + 1.42I_{200}}{I_{110} + 1.42I_{200} + 0.75I_a} \in [0,1] \tag{2}$$

The calculated data were summarized in Table 4.

3.3. SAXS analysis

Fig. 4 shows the Lorentz-corrected SAXS profiles in absolute intensity unit obtained on the same set of samples used in the WAXD measurement. With an assumption of a

Table 3
Comparison of diffraction intensity area and half-peak width of characteristic crystalline peaks for the samples

mLLDPE/LDPE	100/0	80/20	60/40	40/60	20/80	0/100
IA_{110}	1693	7436	7837	7450	7110	1679
IA_{200}	445	1819	1757	1811	1928	467
IA_{110}:IA_{200}	3.80	4.09	4.46	4.11	3.69	3.60
β_{110}	0.60	0.59	0.60	0.59	0.70	0.59
β_{200}	0.77	0.74	0.76	0.77	0.86	0.81
β_{110}:β_{200}	0.78	0.80	0.79	0.77	0.81	0.73

Note: IA represents intensity area here.

two-phase system comprising crystalline and amorphous fractions with distinct interface, the mean long period of the lamellar morphology could be estimated from the maximum value of the scattering vector q_{max} observed in the Lorentz-corrected SAXS scattering profiles.

Based on Bragg's law and the mathematical definition of the scattering vector q, the long period L_B can be calculated from the following equations [23]:

$$L_B = \frac{2\pi}{q_{max}} \tag{3}$$

$$q = \frac{4\pi \sin(\theta/2)}{\lambda} \tag{4}$$

L_B values calculated are listed in Table 4. It is well known that long period L_B reflects the changes in densities for the crystalline and amorphous regions of polymers. As indicated in Table 4, L_B values of the blends take on gradually decreasing tendency as LDPE content increases. The corresponding thickness of the crystalline region (L_c) can be calculated by the following equation:

$$L_c = L_B \chi_c^{WAXD} \tag{5}$$

In the sense that polyethylene belongs to typical orthorhombic crystals, the mean volume of crystallites (V_c) can be calculated as follows:

$$V_c = L_c \times D_{110} \times D_{200} \tag{6}$$

where D is the crystallite size. The number of the crystallites within one volume unit (N_c) can be expressed as follows in a good approximation:

$$N_c \cong \frac{\chi_c}{V_c} \tag{7}$$

Under the assumption of the two-phase model consisting of the alternately stacked structure of the crystalline and amorphous layers, the mean volume of amorphous region (V_a) could be expressed as

$$V_a \cong \left[\frac{(1-\chi_c)}{\chi_c}\right] V_c \tag{8}$$

The parameters of crystalline structure as a function of LDPE content in mLLDPE/LDPE blends are included in Table 4.

As demonstrated in Table 4, the lamellar thickness(L_c, D_{100}, D_{200}), the mean volume of crystallites (V_c) and the mean volume of the amorphous region (V_a) nearly all exhibit decreasing tendency with the increase of LDPE weight fraction; whilst the crystallinity of the blends (X_c) and the crystallites number in one volume unit (N_c) increase as LDPE content increasing, indicating gradually lessened crystal grain size as well as increased crystal grain number. These results further illuminate the influence on mLLDPE crystal structure with the addition of LDPE. Considering the difference in molecular structure for the two kinds of polyethylenes investigated, it is proposed that they possess dissimilar crystallizing ability and crystallinity, which is responsible for the phase separation in the slowly cooling and crystallizing process, and ultimately bring on transformation of the aggregation structure.

On account of the identical chemical composition of mLLDPE and LDPE, their interchain interactions should be the same, whereas the differences in the individual molecular structure decide the characteristics of partial compatibility for mLLDPE/LDPE blend systems. As to binary polyblends with partial miscibility, the discussion below is on the assumption that the dispersed phase spread around the continuous phase in diverse sizes, and compatible region with certain thickness could be formed at the interface, namely, the interface layer. Based upon the experimental results of SAXS, Porod's law [24,25] was employed to obtain the interface layer thickness of the binary systems.

According to Porod's law, for ideal binary system with sharp boundaries, i.e. the fully immiscible two-phase

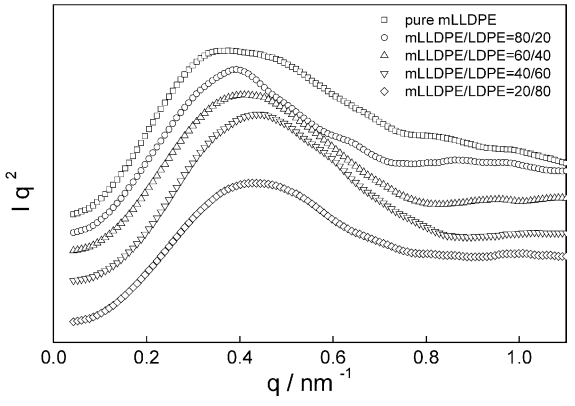

Fig. 4. Lorentz-corrected SAXS profiles of mLLDPE/LDPE blends.

Table 4
Effect of LDPE content on crystalline structure of mLLDPE/LDPE blends

mLLDPE/LDPE	X_c (%)	L_B (nm)	L_c (nm)	L_a (nm)	D_{110} (nm)	D_{200} (nm)	$V_c\times10^{-3}$ (nm^3)	$N_c\times10^4$ (nm^{-3})	$V_a\times10^{-3}$ (nm^3)
100/0	50.3	22.06	11.10	10.96	14.27	11.64	1.84	2.73	1.82
80/20	52.6	21.22	11.16	10.06	14.46	12.02	1.94	2.71	1.75
60/40	53.4	20.16	10.77	9.39	14.28	11.92	1.83	2.91	1.60
40/60	54.0	18.70	10.10	8.60	14.41	11.71	1.70	3.17	1.45
20/80	56.2	18.62	10.46	8.16	11.92	10.54	1.31	4.28	1.02

blends, no affinity exists at the interface, and that the intensity at the tail of the scattering curve is given by Refs. [22,26,27]

$$\lim_{S\to\infty} S^4 I(S) = k \tag{9}$$

where $S=4\pi \sin\theta/\lambda$, $I(S)$ is the intensity of scattering, and k represents Porod constant, which is an important parameter corresponding to the phase structure.

If it is assumed that the interface layer (the compatible domain) exists, Porod's law is given by

$$\lim_{S\to\infty} S^4 I(S) = k\exp(-\sigma_b^2 S^2) \tag{10}$$

where σ_b is the interface layer thickness between the two phases in the blends.

A plot of $\ln S^4 I(S)$ versus S^2 was used and the results are shown in Fig. 5. All the curves appear to be flattened as S increases, and σ_b is calculated by the slope of the tail of the curves, simultaneously k is obtained by the relevant intercept. These results are listed in Table 5. The value of σ_b depends on the composition of the blends, and it is maximum for mLLDPE/LDPE (80/20) blend, corresponding to thick interface layer as well as comparatively uniform structure of the compatible domain, thus the scattering resulting from sharp interfaces is lessened. At the same time, it is proposed that if the tail of the curves are close to level lines, the two phases could be reasonably approximated to be an ideal system, that is to say, fully immiscible in the blends; whilst a larger slope value suggests broader transitional region between the two phases, as well as good miscibility.

SAXS data could be a great help to investigate the morphology of dispersed phase in a multiphase blends [28]. Under the circumstance of regarding the dispersed phase as 'spherical particles', the corresponding scattering intensity $I_S(h)$ can be depicted as

$$I_S(h) \to (\Delta\rho)^2 V 8\pi\bar{l}\frac{1}{h^4} = (\Delta\rho)^2\frac{2\pi}{h^4}S \tag{11}$$

where S is the total interface. Namely, a direct proportion

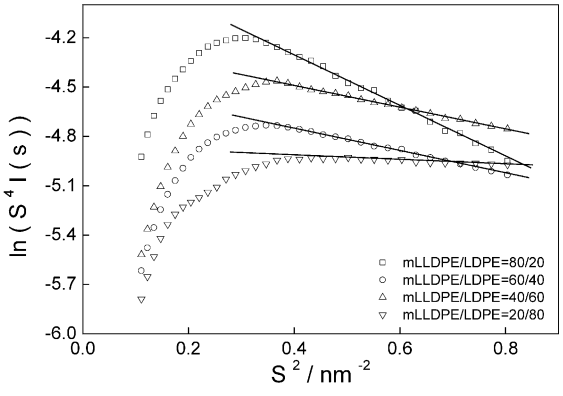

Fig. 5. Plot of $\ln[I(s)\times S^4]$ with S^2 for mLLDPE/LDPE blends.

Table 5
The parameters of phase structure for mLLDPE/LDPE blends

mLLDPE/LDPE	80/20	60/40	40/60	20/80
Porod index α	1.36	1.28	1.31	1.32
Porod constant k	0.026	0.012	0.015	0.018
Interface layer thickness σ_b (nm)	1.26	0.84	0.81	0.35
Correlation distance a_c (nm)	9.44	8.92	8.89	9.21
Integration invariant Q (nm^{-1})	0.023	0.027	0.030	0.023

between $I_S(h)$ and h^{-4} could be drawn, which is a characteristic of 'spherical particles'.

For 'rod-like particles', the corresponding scattering intensity $I_R(h)$ can be depicted as

$$I_R(h) \approx L\frac{\pi}{h}I_C(h) \tag{12}$$

where $I_C(h)$ is the cross-section function. Obviously, a direct proportion between $I_R(h)$ and h^{-1} could be concluded.

For 'flaky particles', the corresponding scattering intensity $I_f(h)$ can be depicted as

$$I_f(h) = A\frac{2\pi}{h^2}I_t(h) \tag{13}$$

$$I_f(h) = (\Delta e)^2\left(\frac{\sinh T/2}{hT/2}\right)^2 \tag{14}$$

where $I_t(h)$ is the cross-section function, and a direct proportion between $I_f(h)$ and h^{-2} could be assumed.

From the above mentioned formulas we might conclude a direct proportion relationship as $I(h) \sim h^{-\alpha}$, wherein α is Porod index. Consequently, as shown in Fig. 6, a plot of $\ln[I(h)]$ against $\ln(h)$ lead to a straight line, and Porod index α could be obtained by the slope of the lines. Summarizing the previous discussions we know that the dispersed phase takes on rod-like morphology under the condition that $\alpha = 1$, whereas $\alpha = 2$ represents flaky morphology, and $\alpha = 4$ represents spherical morphology. As can be seen from Table 5, the Porod index α of all the blends manifest a value range within 1 and 2, and that the changes in α values are not sharp within the whole range of weight fraction. Therefore, it is proposed that in mLLDPE/LDPE blends, the dispersed phase exhibits a transitional state from rod-like to flaky morphology irrespective of the occurrence of phase inversion.

According to the Debye–Bueche statistical theory of scattering from random heterogeneous media [29–31], which gives a relationship concerning spherical symmetrical systems:

$$I(s) = 4\pi K' V_s \bar{\eta}^2 \int_0^\infty \gamma(r)\frac{\sin(hr)}{hr}r^2 dr \tag{15}$$

where V_s is the volume of the scattering unit, $\gamma(r)$ is the correlation function of densities, $h = 4\pi/\lambda \sin\theta$, and $\bar{\eta}^2$ is the mean square amplitude of electronic density, which indicates the uniformity of the blend system investigated and has a relationship with $\gamma(r)$. For polymers, $\gamma(r)$ may be represented by an empirical equation as

$$\gamma(r) = \exp\left(\frac{-r}{a_c}\right) \tag{16}$$

where the parameter a_c is known as a correlation distance and relates to the particle size.

If Eq. (16) is substituted into Eq. (15) one obtains

$$I(s) = 4\pi K' V_s \bar{\eta}^2 \int_0^\infty \exp\left(\frac{-r}{a_c}\right)\frac{\sin(hr)}{hr}r^2 dr \tag{17}$$

Upon integral and rearrangement, it is given by

$$I_s = \frac{4\pi K' V_s \bar{\eta}^2 a_c^3}{(1+h^2a_c^2)^2} = \frac{K'' a_c^3}{(1+h^2a_c^2)^2} \tag{18}$$

Consequently,

$$I_s^{-1/2} = \frac{1}{(K'' a_c^3)^{1/2}}(1+h^2a_c^2) \tag{19}$$

Accordingly, a straight line might be plotted by $I_s^{-1/2}$ against h^2, and a ratio of slope to intercept could lead to the value of a_c. Fig. 7 shows the plot of $I_s^{-1/2}$ with h^2 and relates to the composition of mLLDPE/LDPE blends. The values

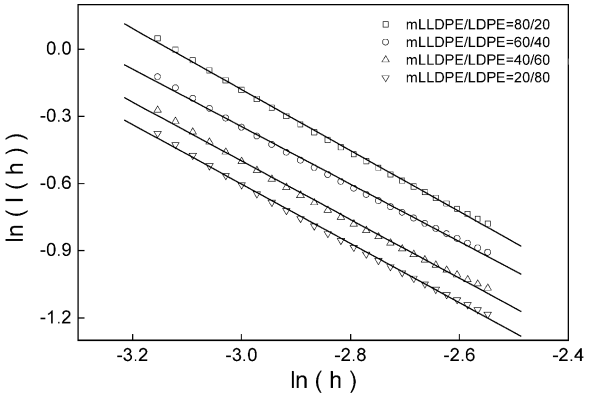

Fig. 6. Plot of $\ln[I(h)]$ with $\ln(h)$ on SAXS for mLLDPE/LDPE blends.

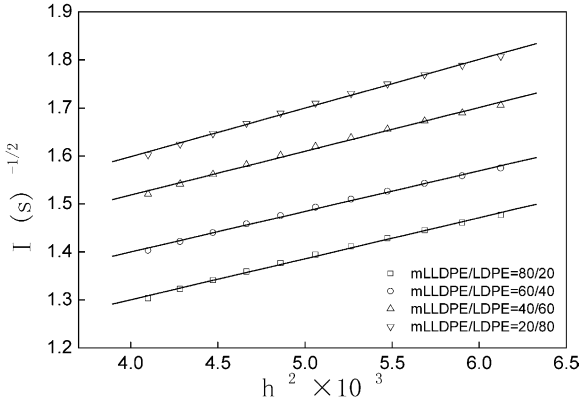

Fig. 7. Plot of $I_s^{-1/2}$ with h^2 on SAXS for mLLDPE/LDPE blends.

calculated are gathered in Table 5. As mentioned above, a_c could represent the correlation size of the dispersed phase. The data in Table 5 show that as LDPE content increases, the values of a_c first decrease slightly, then mount up again. This phenomenon can be rationalized at a microcosmic level. Within the whole weight fractions investigated, there always exists a competition between the two phases, behaving the phase separation in heterogeneity and the aggregation of homogeneities in the blends. At lower LDPE content, it could be reasonably imagined that LDPE is surrounded by the abundance of mLLDPE with high viscosity, and during the blending process the low viscosity LDPE is ripped into smaller flakes. However, in the cooling process, liquid–liquid and liquid–solid phase separation first appears, and in view of the comparatively larger content of mLLDPE chain segments, the occurrence of mLLDPE-rich domains is accompanied by the intensive repulsion towards LDPE segments, making for clear aggregating tendency of LDPE chain segments and that LDPE-rich domains is formed, thus manifesting larger size of the dispersed phase under these circumstances. As LDPE content further increases, the weight ratio between the two components are close to each other, thus the intermolecular entanglement and penetration of the chain segments lead to the formation of entanglement network structure; when the crystalline phase separation arises, the congregating tendency of the dispersed phase is trailed off owing to the interchain disturbance of the repulsion between different chain segments, consequently result in decreased size of the dispersed phase. Ultimately, in the condition that phase inversion occurs, the size of the dispersed phase increase again, just similar to the aforementioned discussion. Thereby, we might sum up that the dispersed phase size is directly related to the phase separation and the aggregation between the two phases.

Additional information may be obtained from the integral invariant (Q), which is related to the degree of phase separation in the blends. It is defined by

$$Q = \frac{\bar{\eta}^2}{K''} = \int I(h)h^2 \mathrm{d}h \tag{20}$$

The values of Q obtained from the integrated SAXS intensity are also listed in Table 5. As a smaller Q value relates to more uniform structure in the blends, a better compatibility is observed both in mLLDPE/LDPE (80/20) and mLLDPE/LDPE (20/80) blends.

4. Conclusions

For mLLDPE/LDPE blends with different weight fractions, the parameters of crystalline structure (i.e. crystallinity and lamellae thickness) as well as parameters of phase structure (i.e. interface layer thickness σ_b, Porod index α, dispersed phase size a_c, integral invariant Q, etc.) were investigated by DSC, WAXD and SAXS experiments. DSC analysis showed the occurrence of cocrystallization in the condition of mLLDPE/LDPE (20/80) blend. As LDPE content decreased, there were two separated peaks during both melting and cooling process, manifested that phase separation occurred in the blends; while the two characteristic peak temperatures came close to each other gradually, indicating the existence of partial cocrystallization. Based on the observed WAXD data, the original orthorhombic crystalline phase has been retained in the blends. Meanwhile, the characteristic of orthorhombic crystals was enhanced as LDPE content increased. SAXS experiment showed that the parameters of phase structure nearly all took on regular changes within the proportional range investigated, relating to the partial compatibility between the two phases, along with lessened size and increased number of crystal grains. Besides, as indicated from the values of Porod index α, the dispersed phase in mLLDPE/LDPE blends is assumed to be in a transitional morphology of rod-like and flaky shapes.

References

[1] Bensason S, Minick J, Moet A, Chum S, Hiltner A, Baer E. J Polym Sci, Part B: Polym Phys 1996;34(7):1301.
[2] Scheirs J, Kaminsky W, editors. Metallocene-based polyolefins, 1st ed, vol. 2. Chichester: Wiley; 2000.
[3] Benedikt GM, Goodall BL, editors. Metallocene catalysed polymers-materials, properties, processing and markets. 1st ed. New York: Plastics Design Library; 1998.
[4] Huang BT, Chen W. Metallocene catalysts and the corresponding polyolefins. Beijing: Press of Chemical Industry; 2000.
[5] Janimak JJ, Stevens GC. J Mater Sci 2001;36:1879.
[6] Bubeck RA. Mat Sci Eng 2002;39(1):1.
[7] Yan D, Wang WJ, Zhu S. Polymer 1999;40(7):1737.
[8] Hatzikiriakos SG. Polym Eng Sci 2000;40(11):2279.
[9] Liu CY, Wang J, He JS. Polymer 2002;43:3811.
[10] Hill MJ, Barham PJ. Polymer 1997;38(22):5595.
[11] Wu T, Li Y, Zhang DL, Tan HM. J Appl Polym Sci 2004;91(2):905.
[12] Ulcer J, Cakmak M, Hsiung CM. J Appl Polym Sci 1996;60:669.
[13] Gahleitner M. Prog Polym Sci 2000;26(6):895.
[14] Krishnamoorti R, Graessley WW, Dee GT, Walsh DJ, Fetters LJ, Lohse DJ. Macromolecules 1996;29:367.
[15] Economou IG. Macromolecules 2000;33:4954.
[16] Wignall GD, Alamo RG, Ritchson EJ, Mandelkern L, Schwahn D. Macromolecules 2001;34(23):8160.
[17] Li YY, Liu CY, Sun X, He JS. Acta Polymerica Sinica 2000;6:707.
[18] Gao JG, Run MT, Wang C, Li ZT, Liu YF. Crystallization behaviour and mechanical properties of the metallocene polyethylene and low density polyethylene blends. 2001 Syposium of polymer, Zhengzhou, China 1995. p. b32.
[19] Liu CY, Li YY, Wang J, He JS. Chem J Chinese Univers 2001;22(2):298.
[20] Tashiro K, Stein RS, Hsu SL. Macromolecules 1992;25:1801.
[21] Datta NK, Birley AW. Plast Rubber Process Appl 1982;2:237.
[22] Yin JH, Mo ZS. Modern polymer physics. Beijing: Science Press; 2001.
[23] Chiu HJ, Chen HL, Lin JS. Polymer 2001;42:5749.
[24] Porod G. Kolloid Z Z Polymer 1952;51:125.
[25] Debye Jr P, Anderson HR, Brumberger H. J Appl Phys 1957;28:679.

[26] Mo ZS, Zhang HF. Structure of crystalline polymers by X-ray diffraction. Beijing: Science Press; 2003.
[27] Sheng J, Ma H, Yuan XB, Yuan XY, Shen NX, Bian DC. J Appl Polym Sci 2000;76:488.
[28] Glatter O, Kratky O. Small angle X-ray scattering. London: Academic Press Inc.; 1982.
[29] Debye P, Bueche AM. J Appl Phys 1949;20:518.
[30] Sheng J, Hu J, Yuan XB, Han YP, Li FK, Bian DC. J Appl Polym Sci 1998;70:806.
[31] Sheng J, Qi LY, Yuan XB, Shen NX, Bian DC. J Appl Polym Sci 1997;64:2265.